

Numerical Study of Haemodynamics in Abdominal Aorta with Renal Branches Using Fluid – Structure Interaction under Rest and Exercise Conditions

Adi Azriff, Cherian Johny, S.M. Abdul Khader, Raghuvir Pai B, M. Zuber, K.A. Ahmed, Zauldin Ahmad

Abstract: Computational simulations studying the complex interaction of blood flow through elastic arteries has demonstrated the haemodynamics of cardiovascular diseases such as atherosclerosis. The aim of present study is to investigate the hemodynamic behavior in 3D models of an idealistic abdominal aorta with renal branches based on (Computed Tomography) CT image. A new technique is used to develop the idealistic model from the single slice. 3D abdominal aorta model with renal branches is generated using ANSYS Design modeler and numerical analysis is performed using FSI solver in ANSYS-17. The blood flow is assumed to be incompressible, homogenous and Newtonian, while artery wall is assumed to behave linearly elastic. The two-way sequentially coupled transient FSI analysis is performed using FSI solver for three pulse cycles. The investigation is focused on haemodynamic parameters such as flow velocity, Wall Shear Stress (WSS), pressure contours, arterial wall deformation and von-Mises stress are studied at the bifurcation and critical zones. The flow variables are monitored throughout pulsatile flow subjected to both resting and exercise cases which is indicated through results obtained. This preliminary study shall be useful to carry out FSI simulation in patient specific cases.

Index Terms: Renal Artery, ANSYS FSI, Exercise and Resting Condition, Normal and High Blood Pressure.

I. INTRODUCTION

The recent developments in computational modelling and simulation have been extensively used to explore the complex interactions of haemodynamics in cardiovascular diseases (Taylor, Hughes and Zarins, 1998). The critical anatomical regions such as arterial bifurcation/ branching or curvature, where complex flow occurs corresponds to locations which are more prone to growth of

atherosclerosis (Fung, 1984). Existing clinical imaging techniques such as Ultrasound Doppler Imaging, Magnetic Resonance Imaging and Computed Tomography have been combined with the numerical simulation techniques such as Fluid-Structure Interaction (FSI) (Kagadis et al., 2008) (Marshall et al., 2004). Such studies have enhanced the understanding of detailed physiology of blood flow in diseased vessels to understand the mechanisms of stenosis development and progression in patients (Ga-Young Suh, et. al., 2011). The flow behavior through normal and healthy artery is quite different in contrast to the stenosed artery with elevated stresses and high resistance to flow. Such study on physiological simulation of flow through stenosis has profound implications for the diagnosis and treatment of vascular disease (Liang, Yamaguchi and Liu, 2006). In contrast to the relatively large number of studies of pulsatile flow in models of the carotid bifurcation and end-to-side anastomosis, there have been few numeric studies of flow in the abdominal aorta (Albert et al., 2014). Anatomically, blood flow in abdominal aorta is crucial as it is one of the largest vessels and further traversing through the abdomen and bifurcating into two legs. Hence, significant portion of the blood from the thoracic aorta flows into the renal arteries and about one-third of the blood flows into the legs under the resting condition (Tang et al., 2006). However, stenosis in renal branch is very important issue as it is linked with secondary hypertension (Albert et al., 2014). In addition, renal stenosis has also demonstrated the pressure & velocity increase and mass flow rate decrease with the higher percentage of stenosis (MOOREJR et al., 1994) (Zhang et al., 2014). The angulation effects of stenosed renal artery based on the velocity of blood and renal mass flow was also investigated (Mortazavinia Z, Arabi S, 2014), which related the cause of hypertension. Similar investigated based on the effect of renal artery stenosis on the vessel wall and flow dynamics based on patient specific data was found in (Kagadis et al., 2008). Its well know fact that, exercise has numerous overall health benefits such as improved cardiorespiratory fitness levels, increased cardiovascular functional capacity and low cardiovascular mortality rates (Amirhossein, et.al., 2015). Eventhough, there are numerous studies which supports the overall benefits of exercise. However, the influence of exercise and mechanism involved in overall improving of arterial health and the intensity and duration of exercise required to maximize the benefit needs more detailed studies (Les et al., 2010).

Manuscript published on 30 December 2019.

*Correspondence Author(s)

Adi Azriff, S.M. Abdul Khader, Zauldin Ahmad, Department of Mechanical Engineering, School of Science and Engineering, Manipal International University, Nilai-71800, Malaysia

Raghuvir Pai B., Department of Mechanical and Manufacturing Engineering, Manipal Institute of Technology, Manipal Academy of Higher Education, Manipal-576104, India

M. Zuber, Department of Automobile and Aeronautical Engineering, Manipal Institute of Technology, Manipal Academy of Higher Education, Manipal-576104, India

K.A. Ahmed, Aerospace Engineering Department, Faculty of Engineering, Universiti Putra Malaysia, Selangor-43499, Malaysia

© The Authors. Published by Blue Eyes Intelligence Engineering and Sciences Publication (BEIESP). This is an open access article under the CC-BY-NC-ND license <http://creativecommons.org/licenses/by-nc-nd/4.0/>

Numerical Study of Haemodynamics in Abdominal Aorta with Renal Branches Using Fluid – Structure Interaction Under Rest and Exercise Conditions

Haemodynamics investigations are carried out during rest and exercise conditions especially in abdominal aorta model for different flow conditions. Flow recirculation zone and low wall shear stress was observed along the posterior wall of the infrarenal abdominal aorta in resting conditions and disappeared during exercise flow conditions (Taylor, Hughes and Zarins, 1999). Flow behavior in light and moderate exercise conditions was compared with rest conditions to highlight the effect of exercise on changes in the flow velocity field and wall shear stress. Idealistic abdominal aorta with peripheral branches, was investigated and compared the regions having low WSS and flow recirculation with previous studies (Lee and Chen, 2002). It was hypothesized that, exercise shall helped in retardation of cardiovascular disease progression by reducing WSS and flow recirculation. However, rest and exercise conditions with more emphasis on renal branches has been limited as observed in previous studies. In addition, effect of normal blood pressure (NBP) and high blood pressure (HBP) on abdominal flow is also limited. In the present study, fundamental investigation is carried out to study the haemodynamics in idealistic abdominal aorta with renal artery branching under resting and exercise condition during NBP and HBP cases.

II. METHODOLOGY

Blood flow in abdominal aorta with renal branch in this study is assumed be to Newtonian, laminar, incompressible and governed by the Navier–Stokes equation for incompressible flows (Pai *et al.*, 2016). Modified momentum equation is adopted in addition to continuity equation as shown in Eq. 1 .

$$\frac{\partial}{\partial t} \int_{\Omega} \rho \delta \Omega + \int_S \rho (v - v_b) \cdot n \delta S = \int_S (\tau_j i_j - P i_i) \cdot n \delta S + \int_{\Omega} b_i \delta \Omega \quad (1)$$

Where ρ is the density, τ is the stress tensor, v is the velocity vector, v_b is the grid velocity, P is the pressure, b_i is the body force at time, t .

Artery wall is assumed to be linearly elastic, isotropic, incompressible and homogeneous (Fung, 1984). Structural solution considering the transient behavior is described by the Eq.2.

$$[M]\{\ddot{U}\} + [C]\{\dot{U}\} + [K]\{U\} = \{F^a\} \quad (2)$$

Where M is the structural mass matrix, C is the structural damping matrix, K is structural stiffness matrix, F_a is the applied load vector and $\{U\}$ represents acceleration, velocity and displacement vector (ANSYS, 2016),(Pai *et al.*, 2016).

Two-way sequentially coupled transient FSI analysis is performed using FSI solver in ANSYS 17.0, a numerical simulation software. FSI solver solves fluid and solid domain separately using ANSYS Fluent and ANSYS Mechanical respectively. Pressure loads from initial ANSYS Fluent solution is transferred to the solid domain through FSI interface and later ANSYS structural domain is solved. Further details of FSI solver are described in detail as observed (ANSYS, 2016).

In the present study, geometry of idealistic abdominal aorta with the renal branches is constructed from a single mid-slice of CT image and the configuration of the model is shown in fig.2. 3D modeling based on CT data is generated in ANSYS Design Modeller. Fig.3 shows the 3D model of normal idealistic abdominal model with renal branches after geometry cleanup and surface refining. Abdominal artery is

highlighted by region 1 and 2, region-3 by left renal artery and region 4 by right renal artery. Fluid region representing artery lumen and solid region representing arterial wall is highlighted by A and B respectively. I\L and O\L represents inlet and outlet respectively. 3D fluid and solid models of abdominal aorta with renal branches are meshed with 85000 and 55000 hexahedral elements. Grid independency study is carried out under steady state condition at early systolic velocity. Flow variables such as velocity, WSS and pressure are monitored by maintaining the grid quality. At inlet and outlet of the fluid model, time varying pulsatile periodic velocity and pressure is applied respectively.

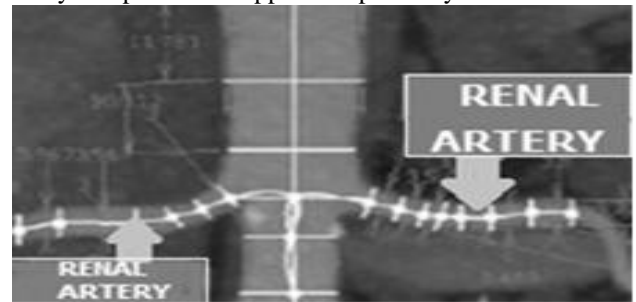


Fig. 2. CT Slice geometry details

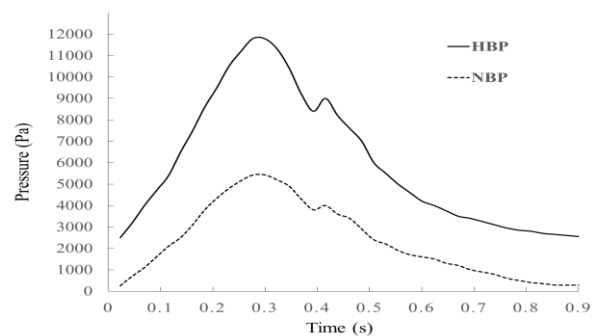


Fig. 3. 3D FSI abdominal aorta model

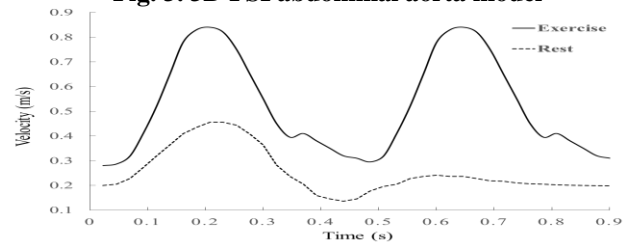


Fig. 5. Pulsatile velocity applied at inlet

In the structural model, both inlet and outlet is fixed in all the directions and rest of the nodes are allowed to get displaced in any direction. The pressure pulse in the descending abdominal aorta is approximately 110-120/70-80 mmHg for a healthy person and 140-200/90-130mmHg in high blood pressure conditions (Khader *et al.*, 2013).

Considering the peripheral resistance offered by the arteries in downstream end, pulsatile pressure waveform is applied at the outlet as shown in the Fig.5 (Zhang *et al.*, 2014). Pulsatile time varying velocity profile as shown in the Fig.5 is applied at the inlet. Two different inlet pulsatile velocities are carried out separately under rest and exercise conditions.

Analysis under the rest condition is performed with pulse cycle of 0.9 sec. In exercise condition, pulse cycle will be 0.5 sec and the flow is observed with two-fold increase as observed in fig.5 (Taylor, Hughes and Zarins, 1999) (Tang et al., 2006). Each pulse cycle during rest and exercise conditions, normal and high blood pressure is discretized into 180 time steps to simulate the flow behavior more accurately. The convergence criteria of fluid flow is set at 10^{-5} and across the fluid-surface interface is set at 10^{-4} respectively. Blood flow and arterial wall properties as observed from (Zhang et al., 2014) and (Khader et al., 2013). Simulation results shall provide useful data in quantifying the haemodynamic changes in understanding the patient specific cases.

III. RESULTS AND DISCUSSION

The haemodynamics parameters like velocity, wall shear stress, pressure, arterial wall deformation and von-Mises stress from FSI simulation are studied from last pulse cycle at specific instants of like early systole, peak systole, early diastole and late diastole.

Velocity: It is observed that velocity profiles are highly different throughout the cardiac cycle. Fig.6 demonstrates the flow velocity profile in abdominal aorta and renal branches. It describes the flow separation such that the flow divides into two streams with maximum velocity at the distal wall of the renal bifurcation and slower moving fluid on the proximal wall (Liang, Yamaguchi and Liu, 2006). Flow separation is found to be more visible during peak systole and deceleration, however later it drops at the diastole phase. These changes in blood flow patterns have been linked to the growth of atherosclerosis. Flow separation are found to be intense closer to the proximal wall in both the renal branches (Mortazavinia Z, Arabi S, 2014).

Flow during peak systole in renal branches is also characterized by the high flow velocity near the distal walls and the low flow velocity near the proximal wall. However, the flow fluctuation is found to be more intense during exercise when compared with rest condition with high flow velocity close to distal walls in both the renal branches as clearly observed from fig.6 (Lee and Chen, 2002) (Les et al., 2010). However, velocity profiles during rest and exercise are similar without any significant changes in both the NBP and HBP cases.

Fig. 7 compares the maximum flow velocity in rest and exercise conditions at different locations such as P1, P2, P3, P4 during cardiac cycle in NBP and HBP cases. It is observed that, flow velocity are not influenced by NBP and HBP in rest and exercise conditions. Higher velocity is observed at upstream side (P1) in abdominal aorta when compared with downstream side (P2). At both these locations (P1 and P2), the flow patterns is similar to inlet pulsatile wave during rest and exercise condition irrespective of NBP and HBP cases. Locations (P3 and P4) demonstrates the disturbed flow profile due to flow recirculation. Wall shear stress (WSS): Results shown in fig.8 depicts that WSS in the abdominal aorta wall tends to increase along its length in upstream side and especially at the branching of renal artery (Liang, Yamaguchi and Liu, 2006) (Lee, Chiu and Jen, 1999).

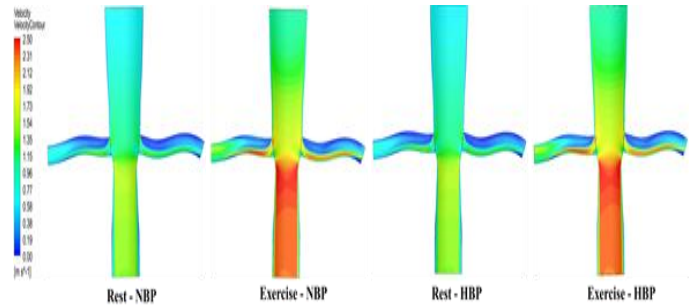


Fig. 6. Comparison of velocity contours in rest and exercise during NBP and HBP

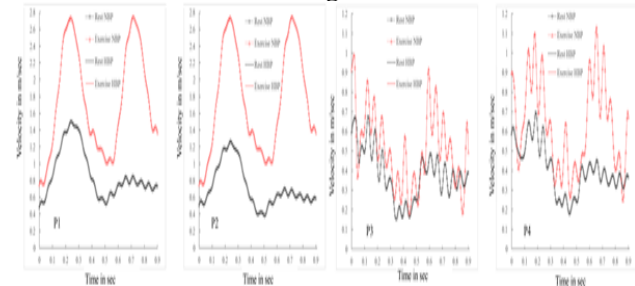


Fig. 7. Comparison of maximum velocity at different locations such as P1, P2, P3 and P4

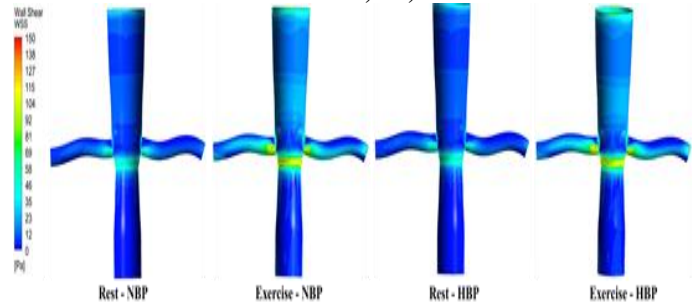


Fig. 8. Comparison of WSS contours in rest and exercise during NBP and HBP

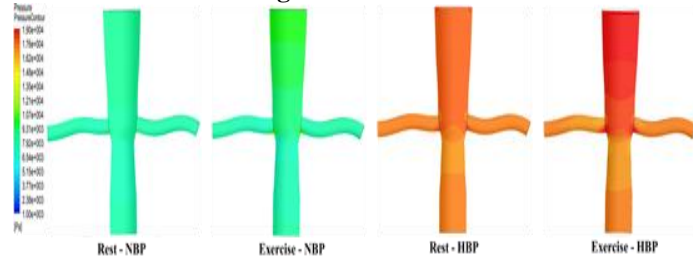


Fig. 9. Comparison of pressure contours in rest and exercise during NBP and HBP

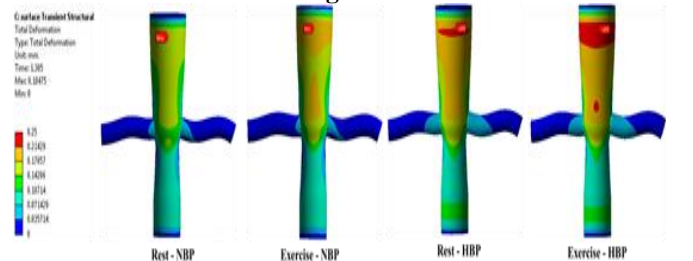


Fig. 10. Comparison of arterial wall deformation in rest and exercise during NBP and HBP

Numerical Study of Haemodynamics in Abdominal Aorta with Renal Branches Using Fluid – Structure Interaction Under Rest and Exercise Conditions

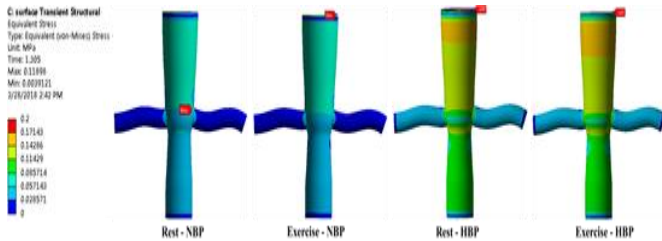


Fig. 11. Comparison of arterial von-Mises stress in rest and exercise during NBP and HBP

At the renal walls, the WSS distribution is found to be low along the proximal wall and the high WSS at the distal renal wall (Taylor, Hughes and Zarins, 1999). The appearance of this low WSS in the proximal wall coincides with the presence of the recirculation. Along the distal wall the WSS will be maximum in the entry of the bifurcation and tends to decrease along the distance. It is also observed that the distal wall in neighbourhood of bifurcation experience high WSS, whereas the proximal walls nearby the flow separation region suffer from relatively low WSS as clearly in fig. 8. Maximum WSS observed at renal bifurcation in distal side is relatively more intense during exercise when compared with rest conditions respectively in both NBP and HBP cases. WSS distribution in distal side extends to larger length in exercise conditions when compared to rest condition influenced by high flow velocity in both NBP and HBP cases.

Pressure: Fig. 9 demonstrates the pressure distribution during peak systole in NBP and HBP case in rest and exercise conditions. Maximum pressure is found to be at the renal bifurcation tip in both branches on distal side during entire cardiac cycle. Upstream abdominal aorta also revealed higher pressure distribution in comparison with downstream side. Exercise condition had higher pressure build up in upstream side of abdominal aorta and at the renal bifurcation tip unlike rest condition as seen from fig.9 during NBP and HBP cases. However, HBP case had larger pressure range over NBP condition as that depicted from outlet pressure profile.

Arterial wall deformation: The total arterial wall deformation behavior is compared in fig.10 during peak systole for rest and exercise conditions during NBP and HBP cases. Maximum arterial wall deformation is found to be during the peak systole, in which the flow is accelerating than compared to the diastole. It is observed that upstream side of abdominal aorta deform significantly unlike downstream side. In NBP case, mild deformation is noticed at entry region of renal artery bifurcation on distal wall side and quite low at proximal wall side which decreases along the distance in rest condition. Similar wall deformation behavior slightly extends to larger length during exercise condition. However, in HBP case, wall deformation behavior extends to larger length during rest and exercise condition. In NBP case, exercise condition has higher wall deformation especially in upstream side of abdominal aorta before branching into renal artery as compared to rest condition. However, in exercise condition during HBP case is observed to depict similar maximum wall deformation behavior in upstream and downstream side of abdominal aorta when compared to rest condition.

Von-Mises stress: Fig. 11 compares the von-Mises stress distribution during peak systole in NBP and HBP during rest and exercise conditions. In cardiac pulse cycle, stress distribution is found to be more visible during peak systole and flow deceleration, however during late diastole stress distribution reduces significantly. Upstream region of

abdominal aorta is found have slightly larger stress distribution unlike downstream side. Stress distribution is found be negligible at the renal artery bifurcation in both the branches in NBP case during rest condition and similar observation during exercise condition. However, in HBP case, mild stress distribution is found to spread the entire renal branches, both in rest and exercise conditions.

IV. CONCLUSION

Numerically simulation of abdominal aorta branching into renal artery using two-way FSI under rest and exercise in NBP and HBP conditions is carried out in this present study. Flow recirculation is observed in proximal side during rest which reduces significantly during exercise condition. Effect of NBP and HBP on renal flow is clearly observed with considerable changes in WSS at renal bifurcation during rest and exercise. Arterial wall deformation and von-Mises stress distribution is found be relatively low at the renal artery bifurcation in NBP case during rest condition and similar observation during exercise condition. However, in HBP case, distribution in renal branches is found to extend along larger distance, in both rest and exercise conditions. The present study is demonstrates the fundamental aspects of haemodynamics in idealized abdominal aorta with renal branches and can be further extended to patient specific cases.

V. ACKNOWLEDGEMENTS

Authors acknowledge the support by Fundamental Research Grant Scheme (FRGS/1/2015/TK03/ MIU/02/1).

REFERENCES

1. Andrea S. Les, Shawn C. Shadden, C. Alberto Figueroa and Charles A. Taylor, 2010. Quantification of Hemodynamics in Abdominal Aortic Aneurysms During Rest and Exercise using Magnetic Resonance Imaging and Computational Fluid Dynamics. *Annals of Biomedical Engineering*, 38(4):1288–1313.
2. Albert Scott, Robert S. Balaban and Jenn Stroud Rossmann, 2014. Influence of the renal artery ostium flow diverter on hemodynamics and atherogenesis. *Journal of Biomechanics*, 47(7):1594–1602.
3. Amirhossein Arzani, Andrea S. Les and Shawn C. Shadden, 2014. Effect of exercise on patient specific abdominal aortic aneurysm flow topology and mixing. *International Journal of Numerical Methods in Biomedical Engineering*, 30(2): 280–295.
4. ANSYS Release 17.0 Documentation, 2016. ANSYS Company, Pittsburgh, PA.
5. Charles A. Taylor, Thomas J. R. Hughes and Christopher K. Zarins, 1998. Finite Element Modeling of Three-Dimensional Pulsatile Flow in the Abdominal Aorta: Relevance to Atherosclerosis. *Annals of Biomedical Engineering*, 26: 975–987.
6. Charles A. Taylor, Thomas J.R. Hughes and Christopher K. Zarins, 1999. Effect of exercise on hemodynamic conditions in the abdominal aorta. *Journal of Vascular Surgery*, 29(6):1077-1089.
7. D. Lee and J.Y. Chen, 2002. Numerical simulation of steady flow fields in a model of abdominal aorta with its peripheral branches. *Journal of Biomechanics*, 35:1115–1122.
8. Ga-Young Suh, Andrea S and Charles A. Taylor, 2011. Hemodynamic Changes Quantified in Abdominal Aortic Aneurysms with Increasing Exercise Intensity Using MR Exercise Imaging and Image-Based Computational Fluid Dynamics. *Annals of Biomedical Engineering*, 39(8):2186–2202.

9. George C. Kagadis, Eugene D. Skouras, Dimitris Karnabatidis and George C. Nikiforidis, 2008. Computational representation and hemodynamic characterization of in vivo acquired severe stenotic renal artery geometries using turbulence modeling. *Medical Engineering & Physics*, 30:647–660.
10. Ian Marshall, Shunzhi Zhao, Peter Hoskins and X Yun Xu, 2004. MRI and CFD studies of pulsatile flow in healthy and Stenosed carotid bifurcation models. *Journal of Biomechanics*, 37:679–687.
11. James E. Moore, Chengpei Xub and David N. Ku. 1994. Fluid wall shear stress measurement in a model of human abdominal aorta: oscillatory behavior and relationship to atherosclerosis. *Atherosclerosis*, 10:225-240.
12. Khader, S. M. A. et al., 2013. Study of the influence of Normal and High Blood pressure on normal and stenosed Carotid Bifurcation using Fluid-Structure Interaction. *Applied Mechanics and Materials*, 315: 982–986.
13. Liang Fuyou, Yamaguchi Ryuhei and Hao Liu, 2006. Fluid Dynamics in Normal and Stenosed Human Renal arteries: an Experimental and Computational Study. *Journal of Biomechanical Science and Engineering*, 1 (1): 171-182.
14. Mortazavinia Z, Arabi S and Mehdizadeh A. R, 2014. Numerical Investigation of Angulation Effects in Stenosed Renal Arteries. *Journal of Biomedical Physics and Engineering*, 4(1):1-8.
15. Raghuvir Pai, et al., 2016. Fluid-Structure Interaction Study of Stenotic Flow in Subject Specific Carotid Bifurcation—A Case Study. *Journal of Medical Imaging and Health Informatics*, 6:1494–1499
16. Tang T Beverly, Cheng P Christoper and Charles A Taylor, 2006. Abdominal Aortic Haemodynamic in young healthy adults at rest and during lower limb exercise: qualification using image-based computer modelling. *American Journal of Heart Circulation Physiology*, 291: H668-676.
17. Weisheng Zhang, Yi Qian and Mengsu Zeng, 2014. Haemodynamic analysis of renal artery stenosis using computational fluid dynamics technology based on unenhanced steady-state free precession magnetic resonance angiography: preliminary results. *International Journal of Cardiovascular Imaging*, 30:367–375.
18. Y. Fung, 1984. *Biodynamics-Circulation*. Springer Verlag, New York Inc.